GLOBAL DISPERSAL OF DUST FOLLOWING IMPACT CRATERING EVENTS ON MARS.

J. Y-K. Cho and S. T. Stewart, Carnegie Institution of Washington, 5241 Broad Branch Rd. NW, Washington, DC 20015, jcho@dtm.ciw.edu, sstewart@gl.ciw.edu.

Introduction. Hypervelocity impacts on Mars inject dust and vapors into the stratosphere. If fine dust and water vapor (derived from the projectile or surface) are globally distributed, impact events could drive transient climate change on Mars [e.g., 1]. Recent work on small impact events (<100 m projectiles) find that the mass of dust stirred into the troposphere may be equivalent to global dust storms [2]. For km-sized impactors, significant amounts of dust may be delivered to the stratosphere. Here, using a simple atmospheric dynamics model, we investigate the global dispersion of dust injected into the stratosphere following large impacts to study the spreading rates, dispersal extent, and the potential for climatic effects.

Model Description. In the stratosphere, motions are predominantly horizontal, due to strong vertical stability. Hence, features whose lateral extent are large compared to the scale height of the atmosphere (~10 km) may be modeled with the shallow-water equations (SWE) [3]. SWE are a vertically-integrated version of the set of primitive equations of meteorology, used in general circulation models. SWE constitute the simplest atmospheric dynamics model which allows the effects of stratification, horizontal compressibility, topography, and differential rotation to be included and studied at high spatial resolution over long simulations times. It has been successfully used in many stratospheric modeling studies for the earth [4-8].

In this study, we restrict our attention to the dispersal pattern of fine (micron-size) particles in the stratosphere and neglect radiative heating/cooling effects and chemistry in the days immediately following a large impact event on Mars. The Mars Orbiter Laser Altimeter (MOLA) topography is included, as it is expected to be important to the flow [9].

We do not consider the morphology of the ejecta plume immediately after the impact. The simulations are initialized with a *post*-impact pressure pulse, 1000 km in radius, radially expanding from the impact site. The shock front is modeled as a large-amplitude height pulse propagating out at 100 m s^{-1} at the edge of the front. This pulse is consistent with several km-sized impactor on Mars. Also present are two, steady geostrophically-balanced zonal jets of amplitude +80 and -80 m s^{-1} at northern and southern mid-latitude, respectively. This is similar to conditions in northern winter (L_S=270-300°) at ~80 km altitude [9].

Results and discussion. We compare the dispersal pattern due to impacts in the northern and southern hemispheres. Figs. 1 and 2 show the evolution of the dispersion pattern for the southern and northern hemisphere case, respectively. The impact site latitude is 30°S and 30°N, respectively, and longitude is 180°W for both cases. Contours of constant dust column density are shown. Note the marked difference in the pattern: the dispersion is limited to a narrow latitudinal band in the northern hemisphere while in the southern hemisphere the dust is spread over wider latitudinal range. This is due to the more complex topography in the southern hemisphere.

We have varied both the strength of the zonal jets and vertical stability (stratification) and observe that this basic behavior does not change qualitatively. In general, the complexity of the dispersal pattern is reduced with weaker jets and is amplified with stronger stratification.

In the future, we will increase the spatial resolution and include more physical effects, such as nonadiabatic heating and gravitational settling.

References. [1] Segura, T.L., et al. (2002) *Science* **298**, 1977-1980. [2] Nemtchinov, I.V., V.V. Shuvalov, and R. Greeley (2002) *JGR* **107**(E12), 5134. [3] Gill, A.E. (1982) *Atmosphere-Ocean Dynamics*, Academic Press: San Diego, p. 95-246. [4] Juckes, M.N. and M.E. McIntyre (1987) *Nature* **328**(6131), 590-596. [5] Salby, M.L., et al. (1990) *J. Atmos. Sci.* **47**(2), 188-214. [6] Norton, W.A. (1994) *J. Atmos. Sci.* **51**(4), 654-673. [7] Polvani, L.M., D.W. Waugh, and R.A. Plumb (1995) *J. Atmos. Sci.* **52**(9), 1288-1309. [8] Otto-Bliesner, B.L. and G.R. Upchurch (1997) *Nature* **385**(6619), 804-807. [9] Richardson, M.I. and R.J. Wilson (2002) *Nature* **416**(6878), 298-301.

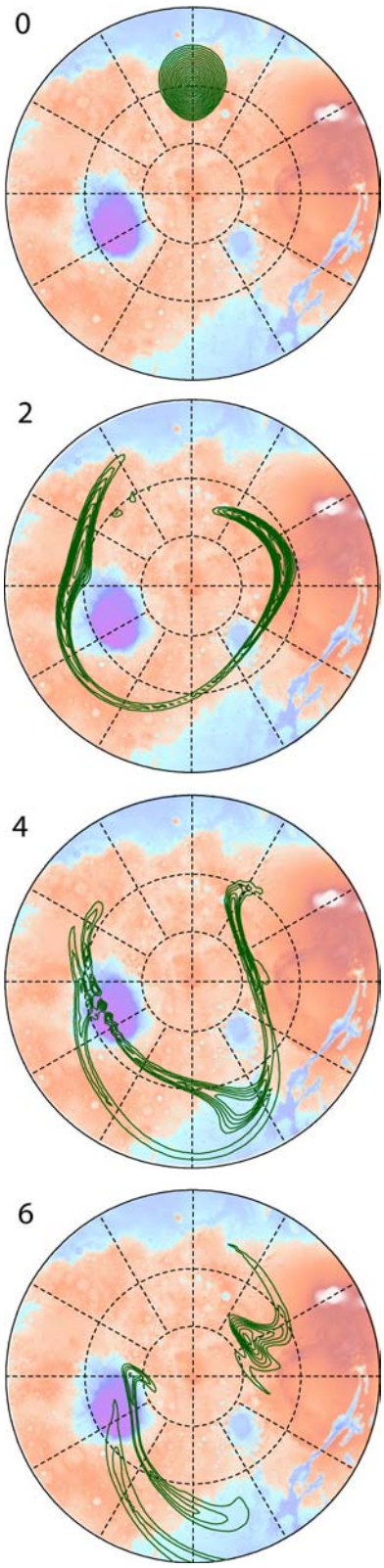

Fig. 1. Density contours of dust dispersal at 2, 4, and 6 Mars days following an impact in the southern hemisphere. Note that the MOLA polar stereographic projection (0 to 90° S) is at higher resolution than the 256×128 grid calculation.

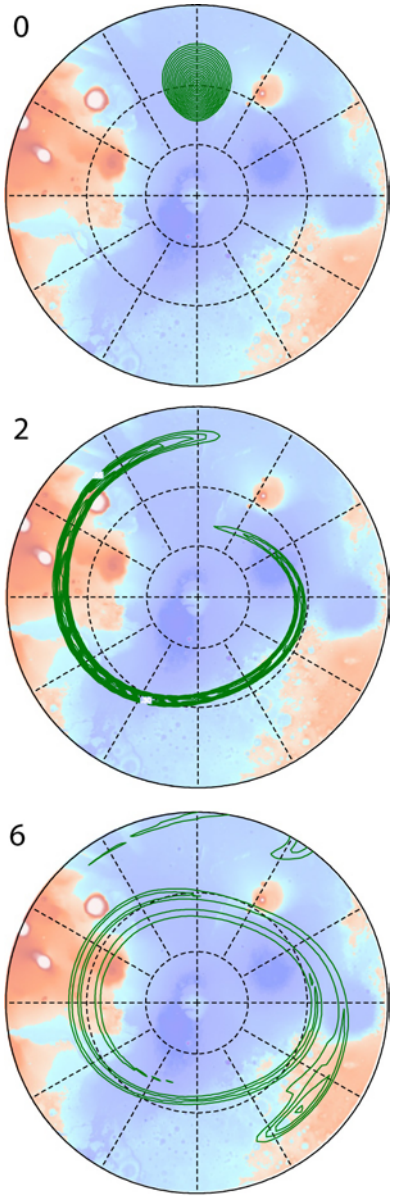

Fig. 2. Density contours of dust dispersal at 2 and 6 Mars days following an impact in the northern hemisphere.